Supplementary Information 1. Assumptions applied in the simulations of ISAV dispersal and their possible implications to the estimation of transmission risk and farm connectivity.

Assumptions	Possible implications
The decay rate of ISAV caused by UV is the same as IHNV	Uncertainty
The decay rate of ISAV caused by the ambient microbial communities is the same as IHNV in the Discovery Islands, BC aquatic environment	Uncertainty
The UV attenuation coefficient in varied water depth is the same as in the Discovery Islands, BC aquatic environment	Uncertainty
ISAV transmission risk within a farm follows a beta-PERT distribution with minimum, mean, and maximum values set as 0.8, 0.9, 0.99, respectively	Overestimate
Shedding rates of ISAV are estimated based on PCR detection results	Overestimate
Each farm has 300,000 fish, with an average weight of 5 kg per fish	Overestimate
All fish in the farm are susceptible to ISAV	Overestimate
No human interventions are included	Overestimate
A farm is considered as one homogeneous cage	Overestimate
No multiple outbreaks occur at the same time	Underestimate
The output of circulation model FVCOM can overall indicate the spatially and temporally varying in the studied region.	Uncertainty
No viral particles lost due to attaching land by applying a land avoidance scheme in PTrack	Overestimate

Supplementary Information 2. Determination of the shedding rate function

Data from a laboratory experiment (Gregory et al. 2009) were used to simulate the shedding rate of ISAV in Atlantic salmon in our modeling framework. In that study, they injected fish with an inoculum of ISAV and monitored the concentration of ISAV every other day in 200 L of water over a 4 h period. Their data showed that viral shedding started around day 7 post-infection, peaked around day 15, and dropped afterward (Table S1.1). We attempted to fit a normal distribution to these data to model the shedding rate of ISAV by Atlantic salmon. The normal distribution function is expressed as:

$$\theta(t) = \frac{\mu}{\sigma\sqrt{2\pi}} \exp\left(-\frac{(t-\beta)^2}{2\sigma^2}\right) \qquad \text{(eq.S1.1)}$$

where θ represents the viral load, t is time in days, μ, β, and σ are coefficients of the normal distribution function, that represent the mean, amplitude, and variance, respectively. Values were obtained using the solver function in EXCEL® software, with: $\beta = 14.18$, $\sigma = 2.94$, and $\mu = 27090335.11$. $R^2 = 0.99$. The figure below shows the form of the normal distribution function overlaid on the raw data (Fig. S2.1). Overall, during the time period covered by the data (days 5 to 19), the function fit the data very well. We note that comprehensive laboratory experiments need be conducted in the future to optimize the function and the coefficients.

Table S2.1. Laboratory experiment of ISAV virus shedding rate

Days post-infection	Shedding rate ($TCID_{50}$ mL^{-1} kg^{-1}) from Gregory et al. (2009)	Deduced Shedding rate ($TCID_{50}$ kg^{-1} h^{-1})*
0	0	0
1	0	0
5	0	0

7	0.058	2,900
11	42	2,100,000
15	70	3,500,000
19	20	1,000,00
21	0	0

*Deduced shedding rate per fish in $TCID_{50}$ kg^{-1} h^{-1} was calculated by modifying the virus shed per fish biomass (in $TCID_{50}$ mL^{-1} kg^{-1}) with the volume of water in fish tank (200 L), then dividing by the shedding time (4 h), according to the method described in Gregory et al. (2009).

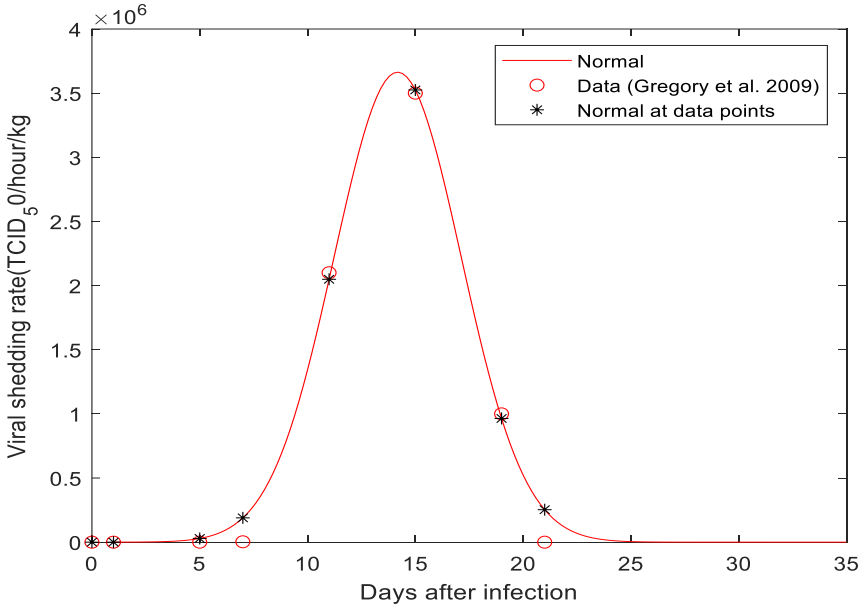

Fig. S2.1 Virus shedding rate model. The normal distribution function is the red line; data from Gregory et al. (2009) are in red circles; modeled values at the data time points of Gregory et al. (2009) are represented by asterisks (*)

Reference

Gregory A, Munro L, Snow M, Urquhart K, Murray A, Raynard R (2009) An experimental investigation on aspects of infectious salmon anaemia virus (ISAV) infection dynamics in seawater Atlantic salmon, *Salmo salar* L. Journal of fish diseases 32:481–489.

Supplementary Information 3. Sensitivity analysis for PTrack time step

The spatial resolution for the physical model (FVCOM) used in this study is as small as 25 m in shallow coastal waters and as large as 11 km in the deeper sea. As the time step retained to simulate particle trajectories was set to 300 s (5 min) in this study, particles could easily move over the smallest grid size of the model during an interval with currents speed exceeding 0.1 m s^{-1}. Hence, the potential of particles jumping over grid cells may degrade the benefits of using a high resolution ocean circulation model and can introduce uncertainties into the particle tracking results.

A finer temporal resolution of 30 s was thus used to repeat the particle tracking simulation and compared with 300 s. To conduct the comparison, two groups of 100 particles were released at Farm 2 every hour for 48 hours, one group tracked at a 30 s time step, and the other at a 300 s time step. Each group of 100 particles was tracked for 24 hours to cover the full tidal and light cycles, and to cover the estimated viral survival time. The mean separation distance was then estimated by first computing the mean trajectory of each group of 100 particles released at each hour from the two model settings (300 s and 30 s), followed by computing the differences between the mean trajectory of the corresponding groups. The mean differences of the 48 groups of particles were then calculated to represent the separation distance of the two model settings.

A single particle from the two groups generally follows the exact same trajectory within 10 hours after release, before separating further over time (Fig. S3.1 for an example). The mean separation distance was estimated for each one of the 48 groups. On average, there was a 24.7 m separation between the two groups three hours after release, and 38.6 m five hours after release (Fig. S3.2). The average variation over the entire tracking time was determined (Fig. S3.2).

Laboratory data suggested that ISAV generally loses its infectivity within three hours in the presence of UV. In this case, the 24.7 m trajectory difference found after three hours tracking between the temporal resolution of 300 s and 30 s is generally within the minimal spatial grid of the ocean circulation

model applied in this study (i.e. 25 m). Thus, the impact of the smaller temporal resolution on the particle trajectory is expected to be low.

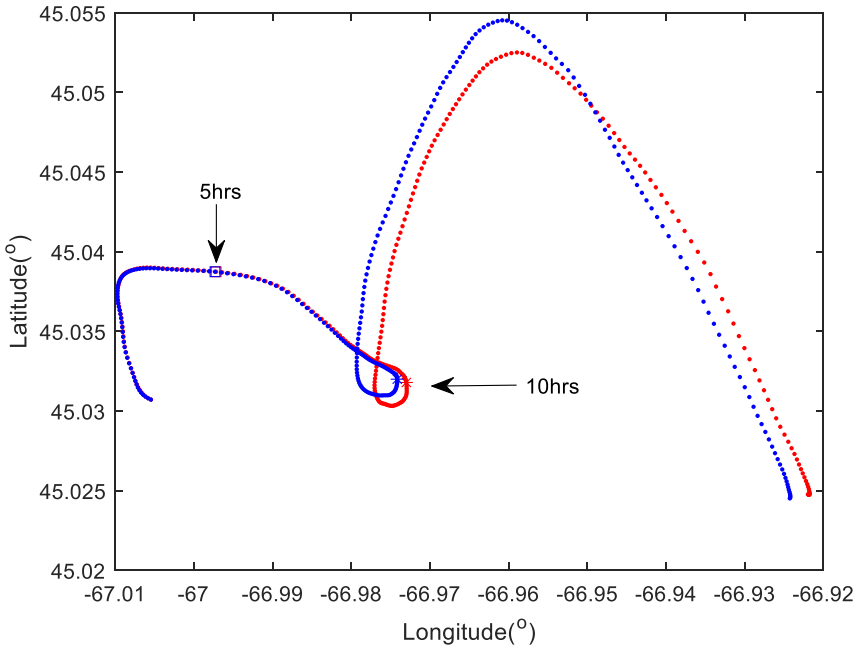

Fig. S3.1 An example of the mean particle trajectory difference of a group of 100 particles simulated with a 300 s (red) and 30 s (blue) time step. Positions of particles at five hours and ten hours after release are indicated.

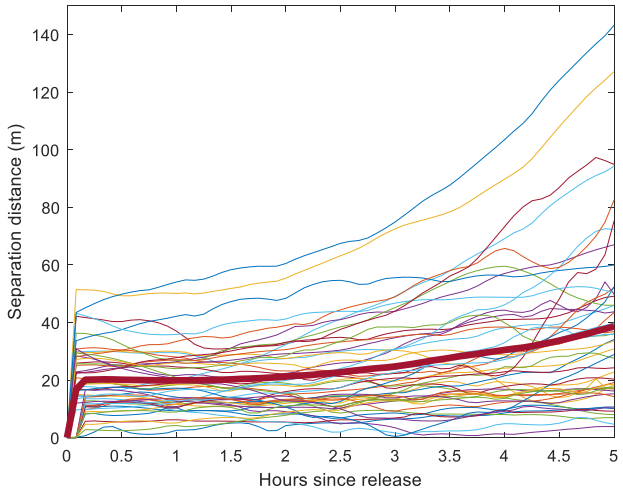

Fig. S3.2 Separation distances between particle groups modeled with the 300 s and 30 s time step, over a tracking time of five hours. Each line represents the differences between the mean trajectories of the corresponding groups from the two model settings (300 s and 30 s), and groups were released every hour for 48 h (100 particles in each group). The bold red curve is the average of all 48 groups of particles.

Table S3.1. Average separation distances between particle groups modeled with a 300 s and 30 s time step, calculated based on groups of 100 particles released hourly for 48 hours (i.e., 100×48 particles), with each group tracked for 24 h.

Hours after release (h)	0	1	2	3	4	5	6	7
Separation distance (m)	0.0	19.9	21.2	24.7	30.5	38.6	48.2	66.3
Hours after release (h)	8	9	10	11	12	13	14	15
Separation distance (m)	87.0	115.0	141.2	164.7	192.8	230.0	281.3	344.5
Hours after release (h)	16	17	18	19	20	21	22	23
Separation distance (m)	424.0	480.9	527.1	577.2	608.3	656.2	698.0	741.4

Supplementary Information 4. Sensitivity analysis for the vertical diffusion coefficient

In this study, the vertical diffusion coefficient for the random walk was set to 0.1 $m^2 s^{-1}$ in the PTrack module. While this parameter can be over 0.1 $m^2 s^{-1}$ in the water near channels and islands, the vertical diffusion coefficient from the outputs of FVCOM indicate that it is likely around 0.01 $m^2 s^{-1}$ in the main part of Passamaquoddy Bay (Fig. S4.1). To demonstrate the impact of the vertical diffusion coefficient on the dispersal of ISAV, we compared the trajectories of particles experiencing vertical diffusion coefficients of 0.01 $m^2 s^{-1}$ and 0.1 $m^2 s^{-1}$. To conduct the comparison, a group of 100 particles were released at Farm 2 every hour for 48 hours. Each group of particles was tracked for 24 hours.

The results indicated that the dispersal scale of the 0.01 $m^2 s^{-1}$group was larger than that of the 0.1 $m^2 s^{-1}$ group (Fig. S4.2). An average difference of 198.4 m was found 3 hours after release, and 333 m at 5 hours after release (Fig. S4.3). These results indicate that the vertical diffusion coefficients may impact the trajectory results substantially, and higher vertical diffusion can result in an underestimation of the horizontal particle dispersion.

Given that most farms are scattered in the higher vertical diffusion area, we considered 0.1 $m^2 s^{-1}$ to be acceptable for our main simulations. Although it seems logical to apply a dynamic vertical diffusion coefficient, such as one determined from the ocean circulation model, to better capture the spatial variation of the vertical turbulent mixing of the area, applying a fixed space-independent value does provide flexibility for optimal modelling performance (Page et al. 2005). The vertical diffusion coefficient impacts the depth of particles, which can impact the UV attenuation process in our inactivation module. Viral concentration can be impacted due to UV degradation at different depths. To demonstrate how the vertical diffusion coefficient impacts the viral concentration, a comparison between the 0.01 $m^2 s^{-1}$ and 0.1 $m^2 s^{-1}$ groups was produced (Fig. S4.4). The results indicated that, although the dispersal scales were larger for the 0.01 $m^2 s^{-1}$ group, the viral concentration near the farm area was relatively lower for this group compared with the 0.1 $m^2 s^{-1}$ group. Besides the potential dilution effects caused by wider dispersion, the lower concentration can be explained by particles likely being closer to the water surface

with a lower vertical diffusion, which enhanced their decay by UV radiation. Consequently, on the daily concentration map, less virus were infectious in this case.

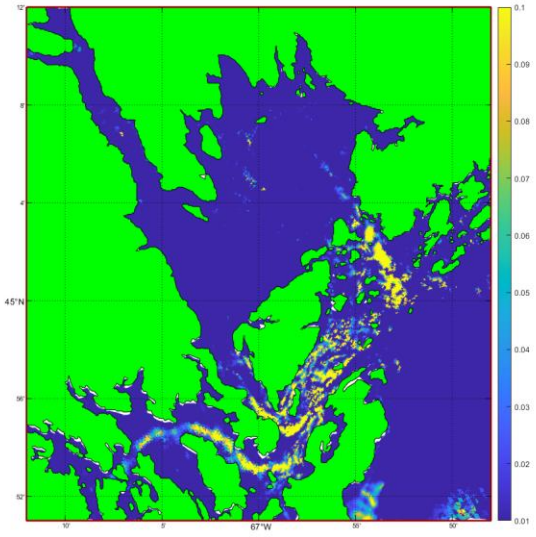

Fig. S4.1 Simulated vertical diffusion coefficients of the surface layer, retrieved from the FVCOM output. Colors on the map represent the values of the modeled vertical diffusion coefficient. (Note: Farms 1, 2, and 4 are in the area with lower vertical diffusion coefficients, and the other 10 farms are in areas with higher vertical diffusion coefficients).

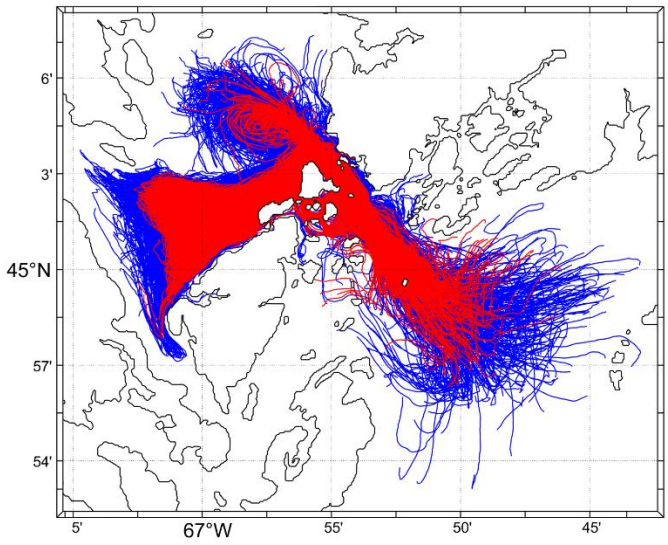

115

116 **Fig. S4.2** Trajectory differences for particles simulated at different vertical diffusion coefficients: 0.1 m^2

117 s^{-1} (red) and 0.01 m^2 s^{-1} (blue) during 48 hours of tracking.

118

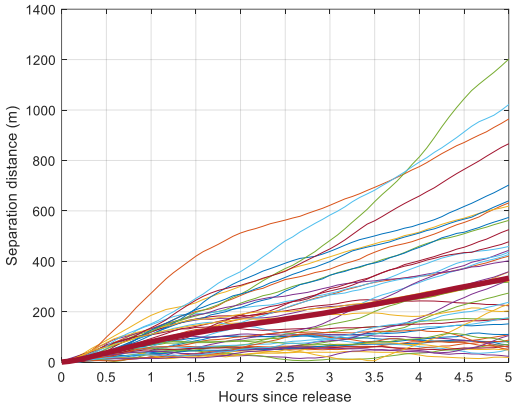

119

120 **Fig. S4.3** Distances separating particle groups with different vertical diffusion coefficients over a tracking

121 time of 5 hours. Each line represents the differences between the mean trajectory of the corresponding

122 groups from the two model settings (0.1 m^2 s^{-1} and 0.01 m^2 s^{-1}), as one of 48-hourly released groups (100

123 in each group). The bold red curve is the average of all 48 groups of particles.

124

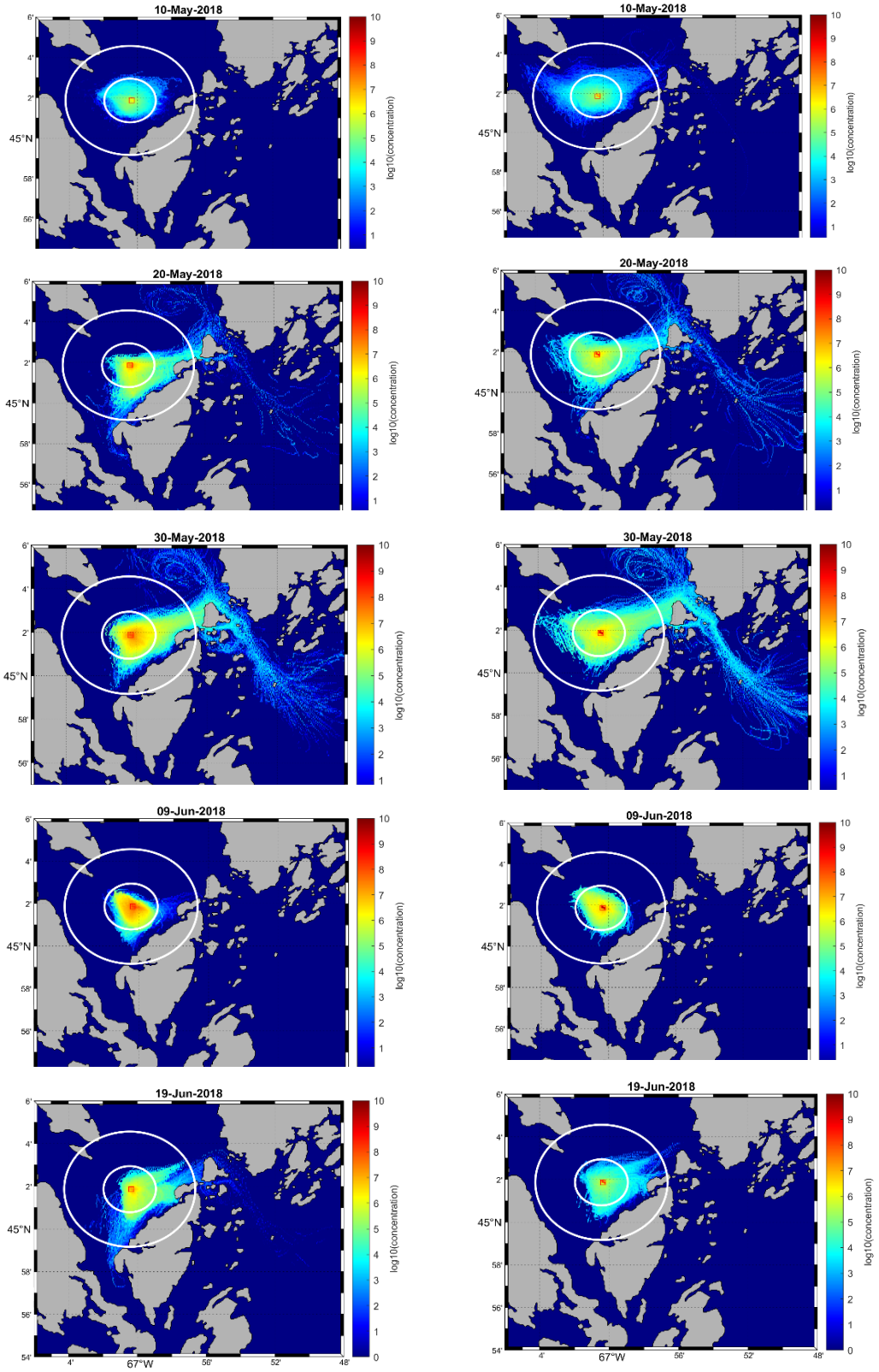

A :0.1 $m^2 \cdot s^{-1}$

B :0.01 $m^2 \cdot s^{-1}$

Fig. S4.4 ISAV concentration ($\log_{10}(TCID_{50}\ m^{-3})$) released from Farm 2 in the top 15 m of the water column and summed over a 24-h period on different days (10, 20, 30, 40, 50 days) post-outbreak and simulated with different vertical diffusion coefficients. A side: 0.1 $m^2\ s^{-1}$ and B side : 0.01 $m^2\ s^{-1}$. The red square represents Farm 2 location. The radii of the two white circles centered at Farm 2 are 2 km and 5 km, respectively.

References

Page FH, Chang B, Losier R, Greenberg D, Chaffey J, McCurdy E (2005) Water circulation and management of infectious salmon anemia in the salmon aquaculture industry of southern Grand Manan Island, Bay of Fundy, Canada. Canadian Technical Report of Fisheries and Aquatic Sciences 2595.

Supplementary Information 5. UV radiation conversion

The viral decay caused by ultraviolet light is mainly from the UV_A (315-400 nm) and UV_B (280-315 nm) bands (Garver et al. 2013; Häder et al. 2015). However, direct measurements of UV radiation were not available for the studied area. Hence, we used a UV index from the closest available operational UV monitoring station from Environment Canada, in Toronto, Ontario (Canada). (Data available at: https://exp-studies.tor.ec.gc.ca/). The UV index is an irradiance scale computed by multiplying the erythemal irradiance (286.3-363 nm) integral in Watts m^{-2} by 40 (McKinley and Diffey 1987).

It should be noted though that the UV index covers a narrower range of wavelengths compared to UV_A and UV_B. As a result, the UV index was converted to total UV radiation using the empirical equation provided by Foreman et al. (2015) based on an experiment conducted by Garver et al. (2013) using a Davis UV sensor (#6490) that measured erythemal UV (280 to 360 nm, the UV Index) and a Davis solar radiation sensor (#6450) that measured total solar radiation (110 to 400 nm) as:

$$UV_{AB}\ (W\ m^{-2}) = (a1 \times UV_{index} \times 0.025 + b1) \times (1 - 0.08) \qquad \text{(eq. S5.1)}$$

where the UV index was multiplied by 0.025 to get the erythemal UV radiation (W m^{-2}); a1 = 302.8926, b1 = 3.6671.

It must be noted that the empirical relationship between the UV index and UV radiation can vary with different atmospheric parameters, e.g., ozone profile, aerosol properties, and Solar Zenith Angle (Allaart et al. 2004), as well as with the experimental conditions. In addition, ocean albedo may be adjustable, as the average ocean albedo was reported to be between 0.05 and 0.10 (Seitz 2011). These introduce some uncertainties for the calculation of UV radiation applied in our current model. Measurements of the incident UV radiation in the local area of our study is needed to better estimate the viral decay caused by UV.

References

Allaart M, van Weele M, Fortuin P, Kelder H (2004). An empirical model to predict the UV-index based on solar zenith angles and total ozone. Meteorological Applications 11:59-65.

Garver KA, Mahony AA, Stucchi D, Richard J, Van Woensel C, Foreman M (2013) Estimation of parameters influencing waterborne transmission of infectious hematopoietic necrosis virus (IHNV) in Atlantic salmon (*Salmo salar*). PLoS One 8:e82296.

Häder D-P, Williamson CE, Wängberg S-Å, Rautio M, Rose KC, Gao K, Helbling EW, Sinha RP, Worrest R (2015) Effects of UV radiation on aquatic ecosystems and interactions with other environmental factors. Photochemical and Photobiological Sciences 14:108–126.

McKinlay AF and Diffey BL (1987) A reference action spectrum for ultraviolet induced erythema in human skin. pp. 83-87 in Passchier WF, Bosnjakovic BFM [eds]. Human Exposure to Ultraviolet Radiation: Risks and Regulations, Elsevier, Amsterdam.

Seitz R (2011) Bright water: hydrosols, water conservation and climate change. Climatic Change 105:365-381.

Supplementary Information 6. Sensitivity analysis for the size of secondary grid cells

To facilitate the calculation and visualization of particle concentrations, we applied a secondary grid different from that of the particle tracking output generated by PTrack. It should be noted that this secondary grid does not affect the particle tracking results, but could have an effect on the estimated concentration in some areas. To test how the selection of the secondary grid cell size impacts viral concentration calculation, we compared the results obtained when using a larger grid size (i.e., 200 m ×200 m) to the one retained for our analyses (i.e., 135 m ×47 m). The viral tracking results of Farm 2 were used as an example for this sensitivity analysis. A daily map of May 30, 2018 was produced for illustration purposes (Fig. S6.1).

The viral concentration map created with the 200m × 200m secondary grid resulted in a more spatially continuous distribution. However, given the large number of particles released, i.e., 100 particles at each hour for 55 days, the current 135 m × 47 m secondary grid was also able to provide a similar continuity, with comparable concentration values shown on the maps.

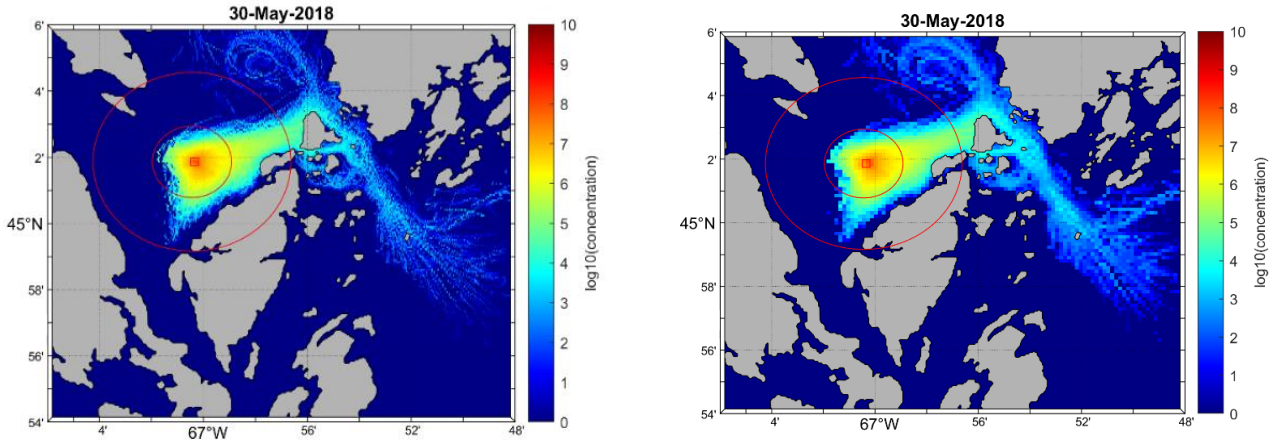

A: 135 m x 47 m grid

B: 200 m x 200 m grid

Fig. S6.1 Average daily ISAV concentration ($\log_{10}(TCID_{50} \cdot m^{-3})$) released from Farm 2 over the top 15 m of the water column at day 30 post-outbreak and using two different secondary grids. A: 135 m × 47 m and B: 200 m × 200 m. The radii of the two red circles centered at Farm 2 are 2 km and 5 km, respectively.

Supplementary Information 7. Concentration maps for all selected farms

Daily dispersal maps with the average viral load over the top 15 m of the water column were produced for all selected farms following a simulated outbreak, and are posted below to provide the reference ISAV dispersal predictions from our framework.

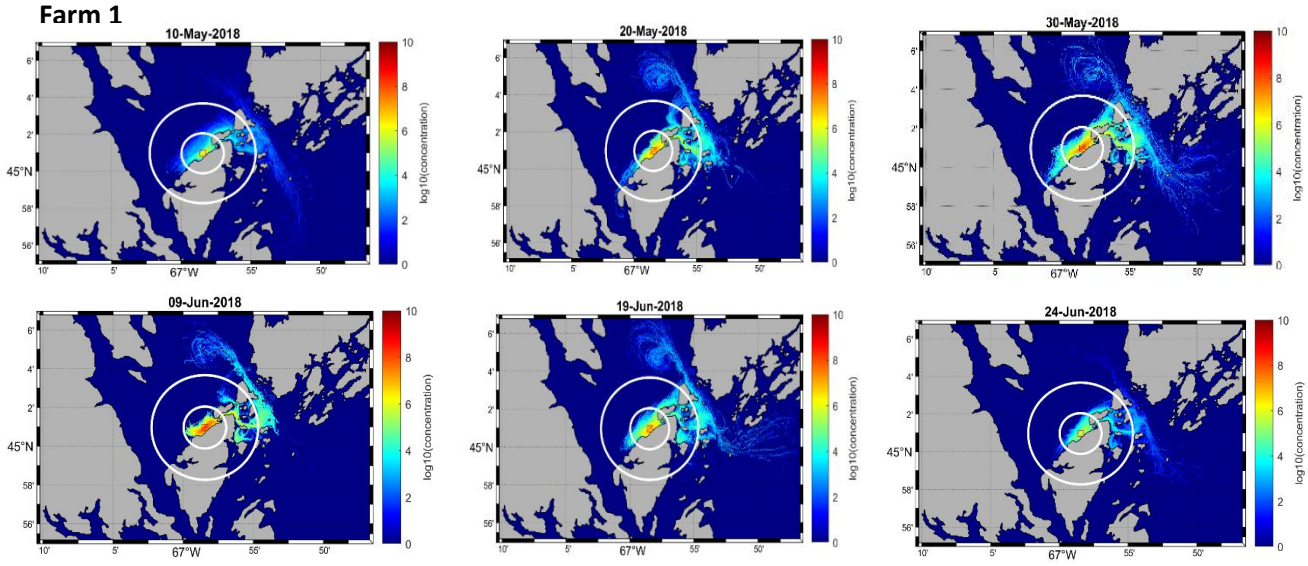

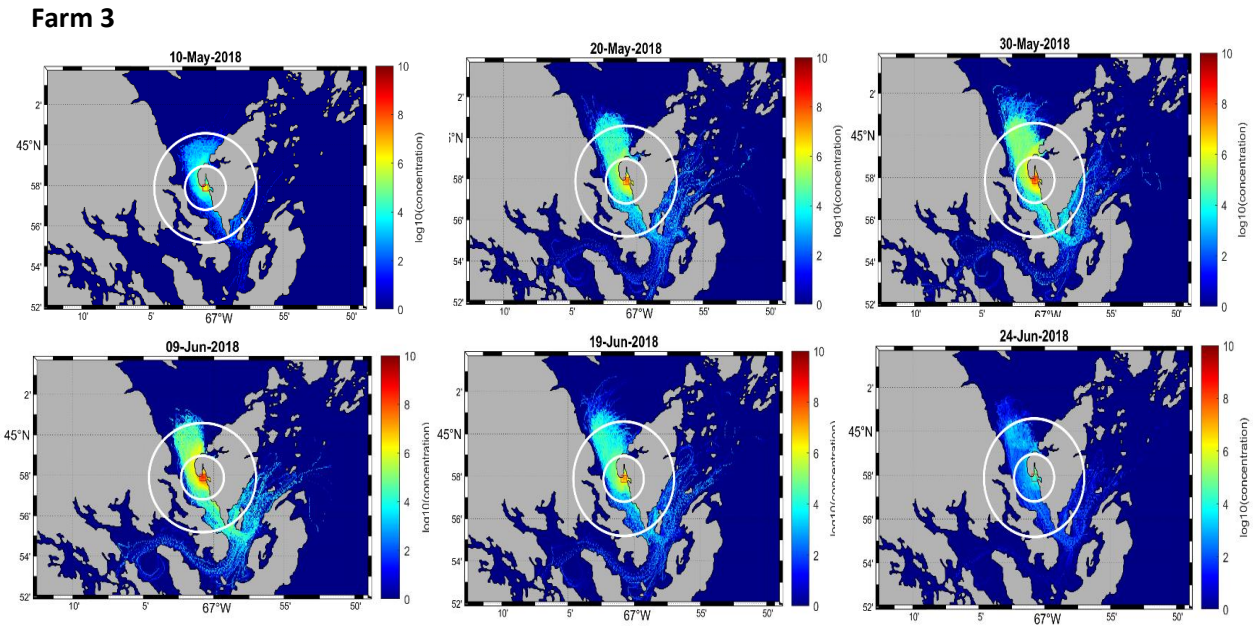

Farm 4

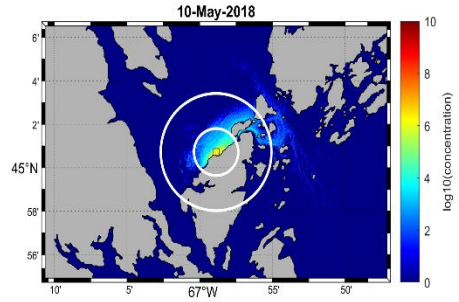
10-May-2018
45°N
67°W
log10(concentration)

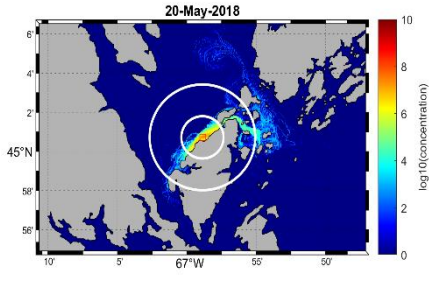
20-May-2018
45°N
67°W
log10(concentration)

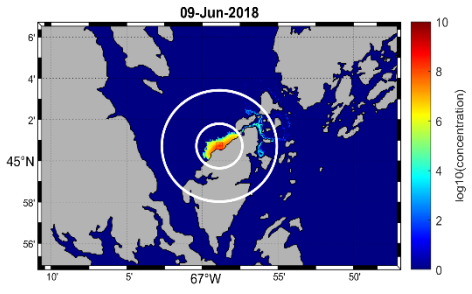
09-Jun-2018
45°N
67°W
log10(concentration)

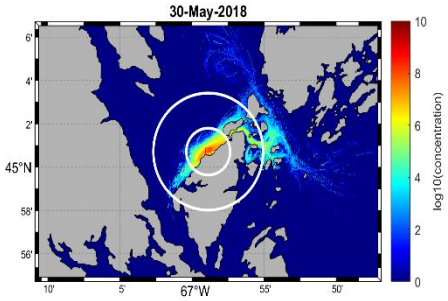
30-May-2018
45°N
67°W
log10(concentration)

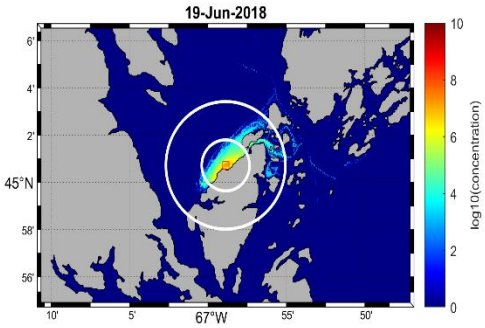
19-Jun-2018
45°N
67°W
log10(concentration)

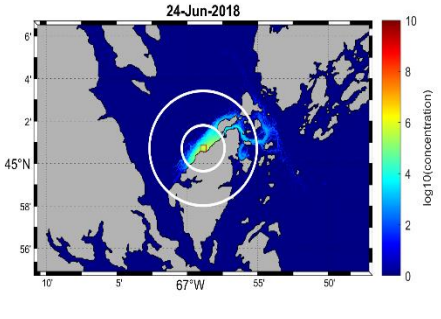
24-Jun-2018
45°N
67°W
log10(concentration)

Farm 5

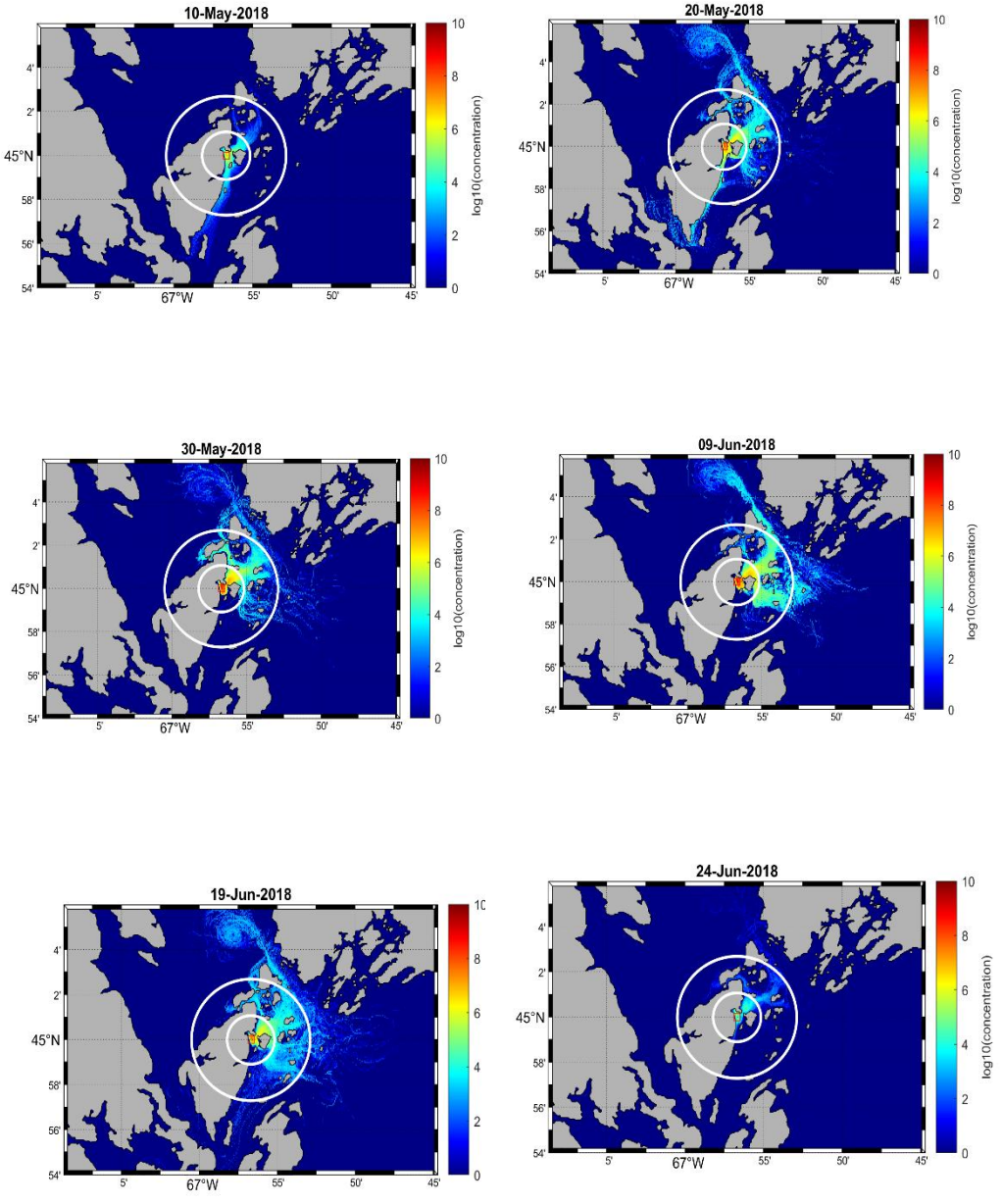
10-May-2018
20-May-2018
30-May-2018
09-Jun-2018
19-Jun-2018
24-Jun-2018
45°N
67°W
log10(concentration)

Farm6

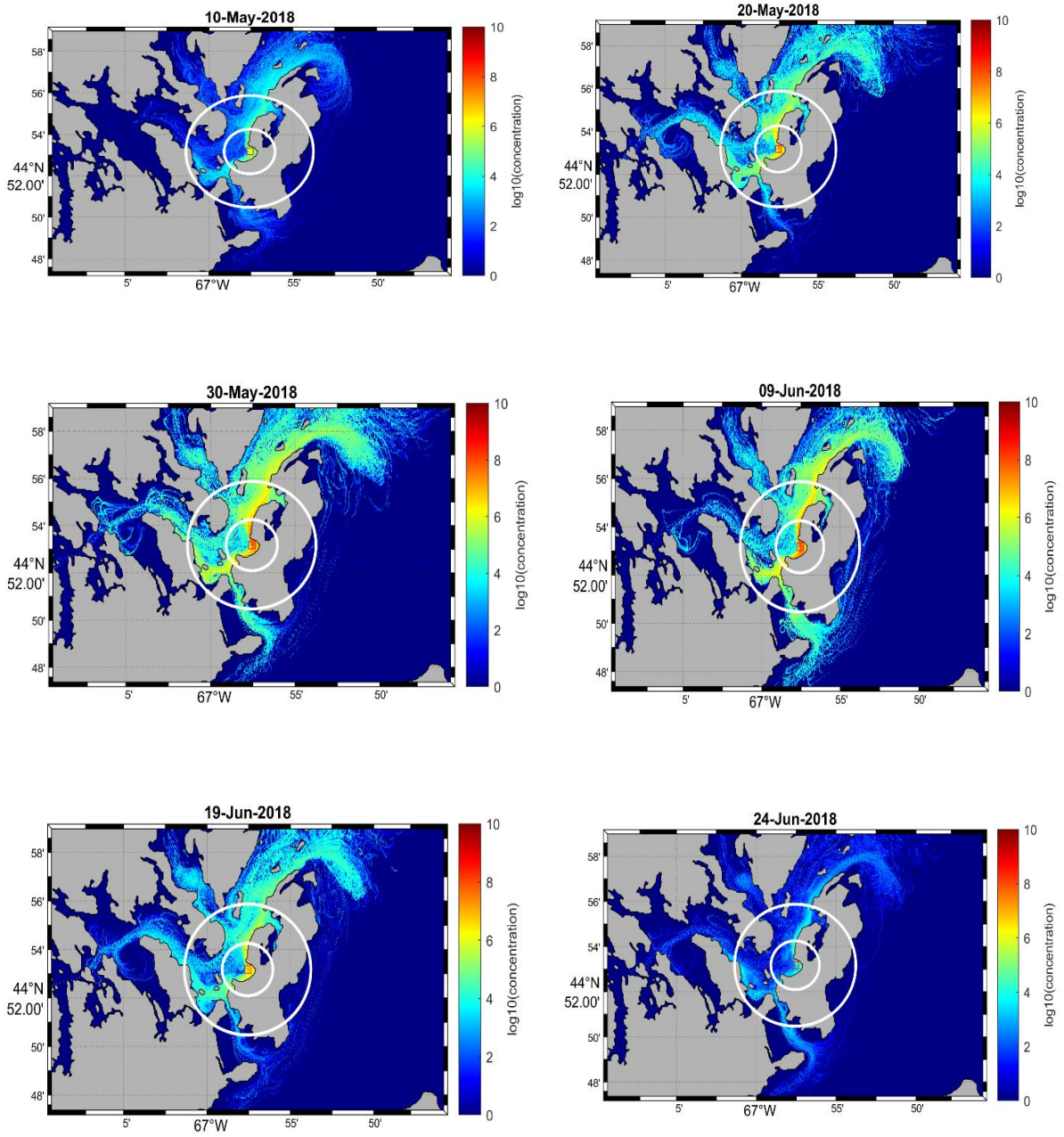
10-May-2018
20-May-2018
30-May-2018
09-Jun-2018
19-Jun-2018
24-Jun-2018
log10(concentration)
44°N
52.00'
67°W

Farm 7

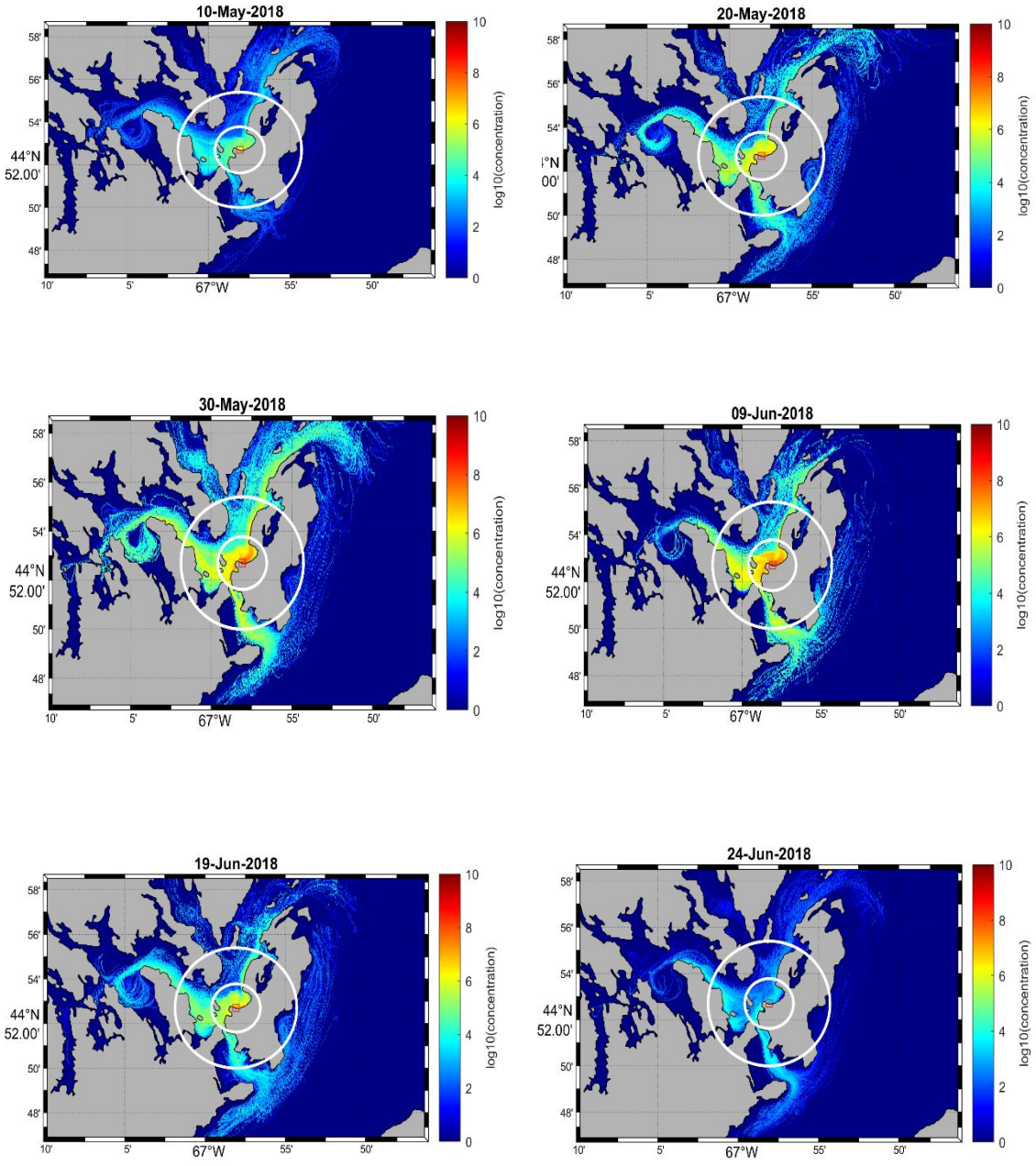
10-May-2018
20-May-2018
30-May-2018
09-Jun-2018
19-Jun-2018
24-Jun-2018
log10(concentration)
67°W
44°N
52.00'

Farm 8

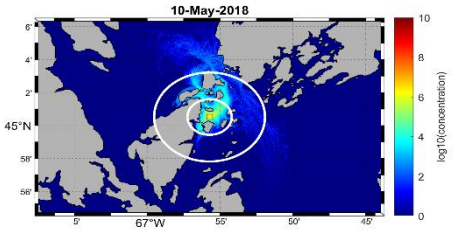
10-May-2018
45°N
67°W
log10(concentration)

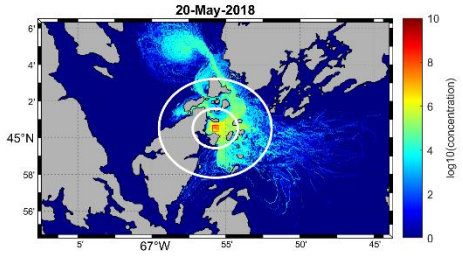
20-May-2018
45°N
67°W
log10(concentration)

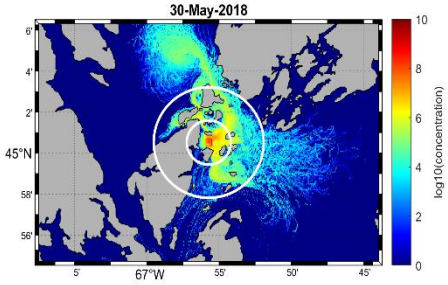
30-May-2018
45°N
67°W
log10(concentration)

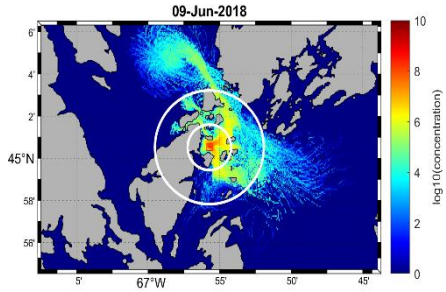
09-Jun-2018
45°N
67°W
log10(concentration)

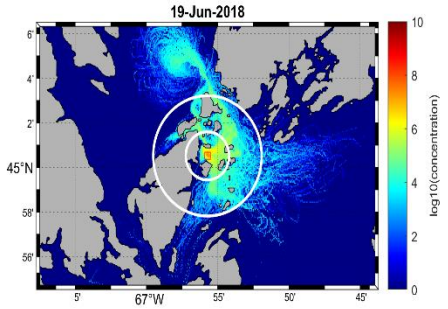
19-Jun-2018
45°N
67°W
log10(concentration)

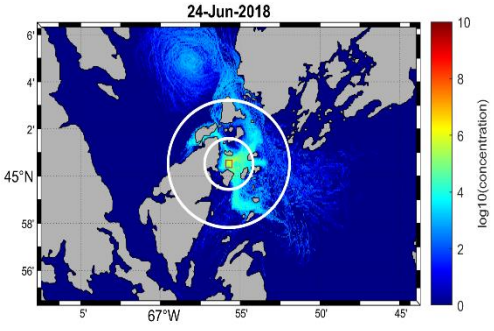
24-Jun-2018
45°N
67°W
log10(concentration)

Farm 9

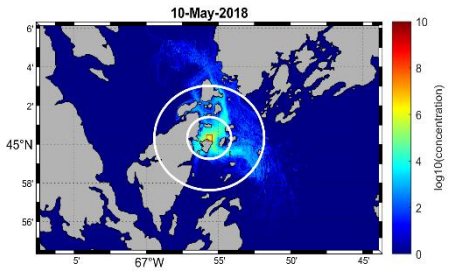
10-May-2018
45°N
67°W
log10(concentration)

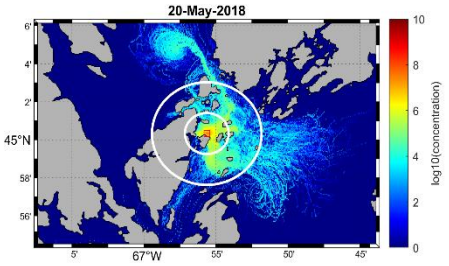
20-May-2018
45°N
67°W
log10(concentration)

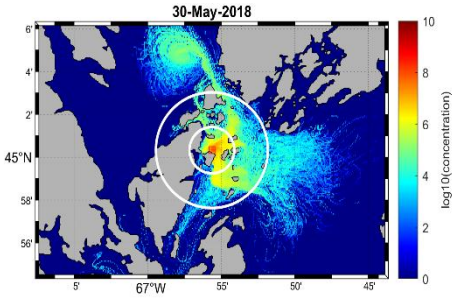
30-May-2018
45°N
67°W
log10(concentration)

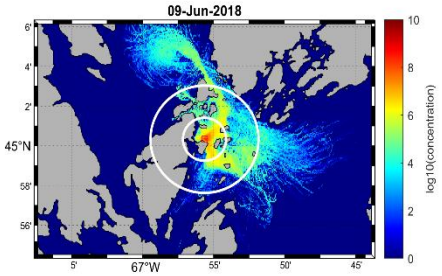
09-Jun-2018
45°N
67°W
log10(concentration)

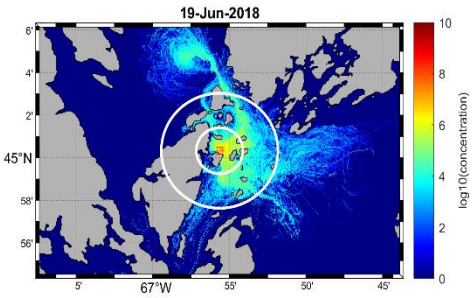
19-Jun-2018
45°N
67°W
log10(concentration)

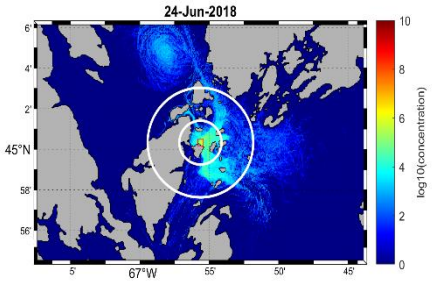
24-Jun-2018
45°N
67°W
log10(concentration)

Farm 10

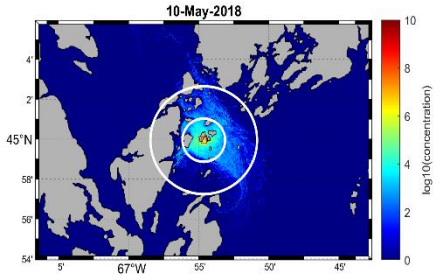
10-May-2018
45°N
67°W
log10(concentration)

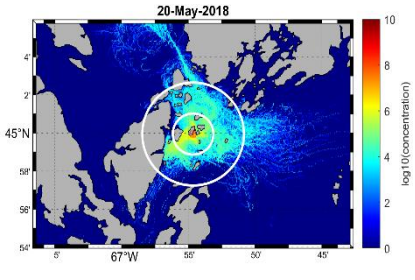
20-May-2018
45°N
67°W
log10(concentration)

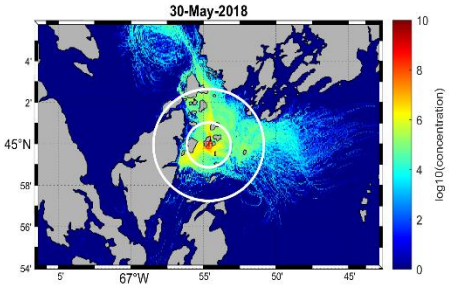
30-May-2018
45°N
67°W
log10(concentration)

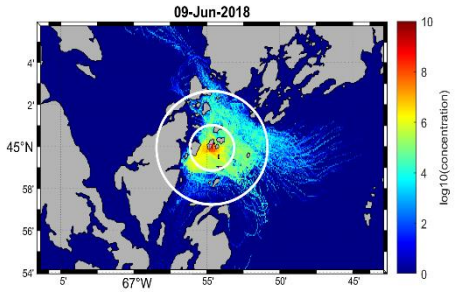
09-Jun-2018
45°N
67°W
log10(concentration)

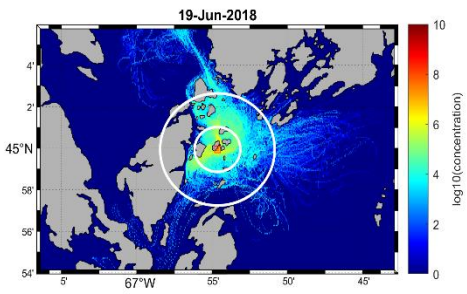
19-Jun-2018
45°N
67°W
log10(concentration)

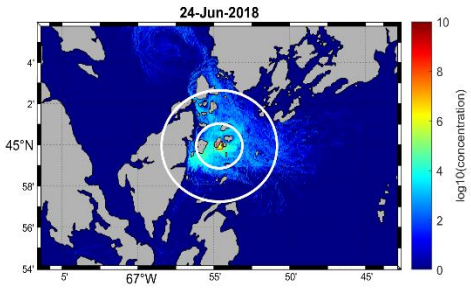
24-Jun-2018
45°N
67°W
log10(concentration)

212

Farm11

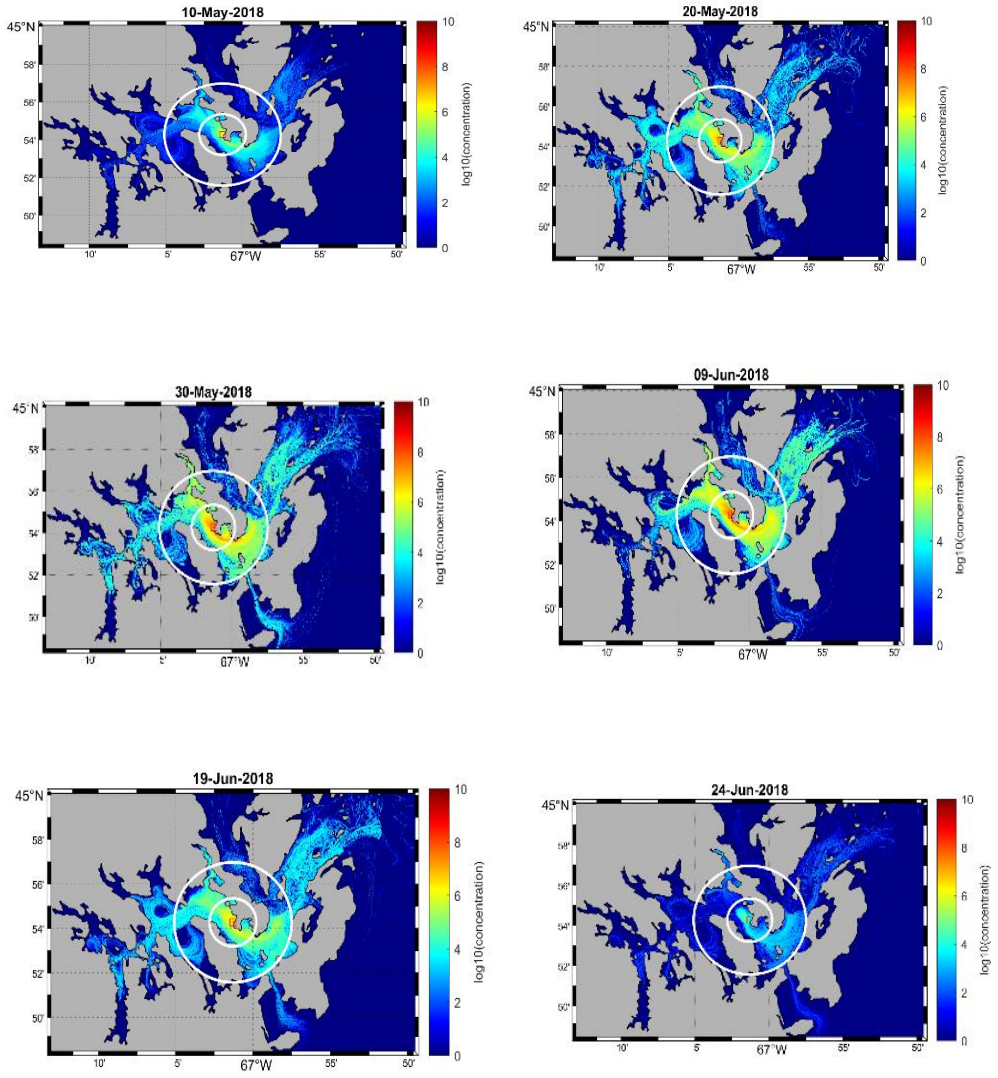

213

214

Farm12

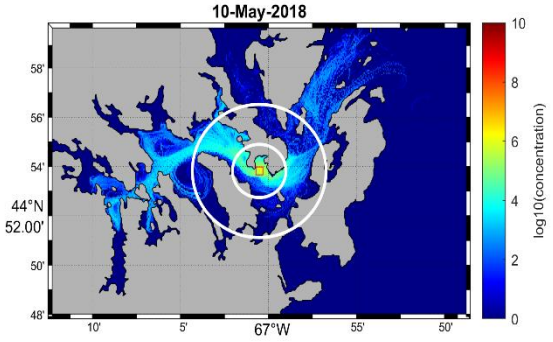
10-May-2018
58'
56'
54'
44°N
52.00'
50'
48'
10'
5'
67°W
55'
50'
10
8
6
4
2
0
log10(concentration)

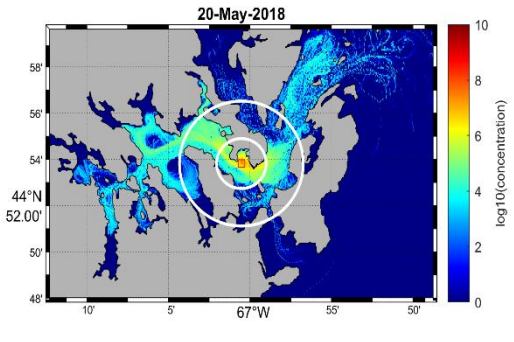
20-May-2018
58'
56'
54'
44°N
52.00'
50'
48'
10'
5'
67°W
55'
50'
10
8
6
4
2
0
log10(concentration)

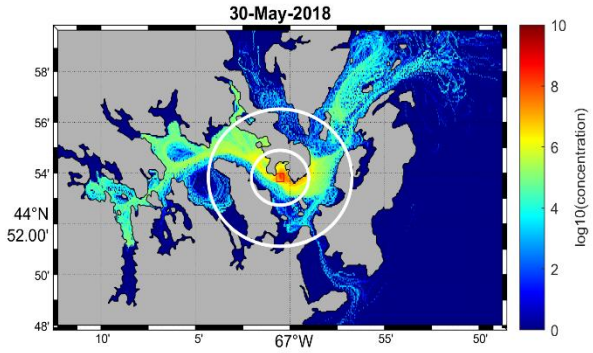
30-May-2018
58'
56'
54'
44°N
52.00'
50'
48'
10'
5'
67°W
55'
50'
10
8
6
4
2
0
log10(concentration)

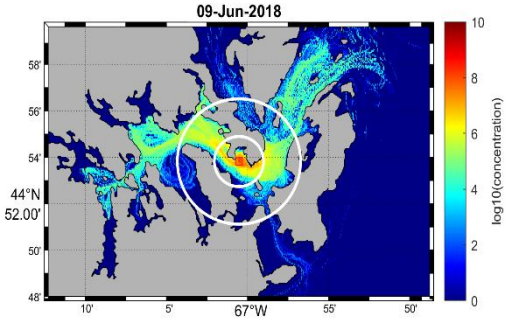
09-Jun-2018
58'
56'
54'
44°N
52.00'
50'
48'
10'
5'
67°W
55'
50'
10
8
6
4
2
0
log10(concentration)

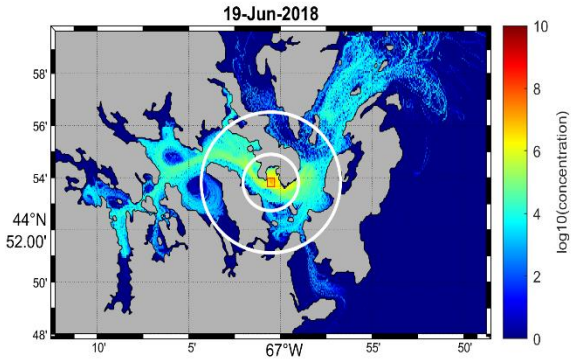
19-Jun-2018
58'
56'
54'
44°N
52.00'
50'
48'
10'
5'
67°W
55'
50'
10
8
6
4
2
0
log10(concentration)

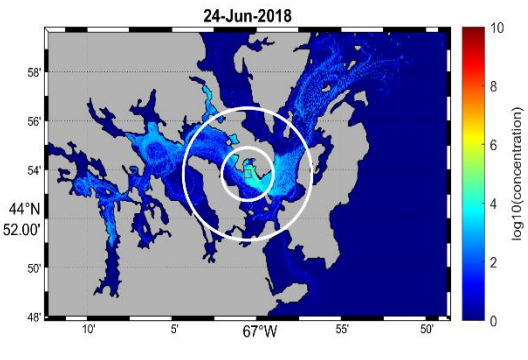
24-Jun-2018
58'
56'
54'
44°N
52.00'
50'
48'
10'
5'
67°W
55'
50'
10
8
6
4
2
0
log10(concentration)

Farm13

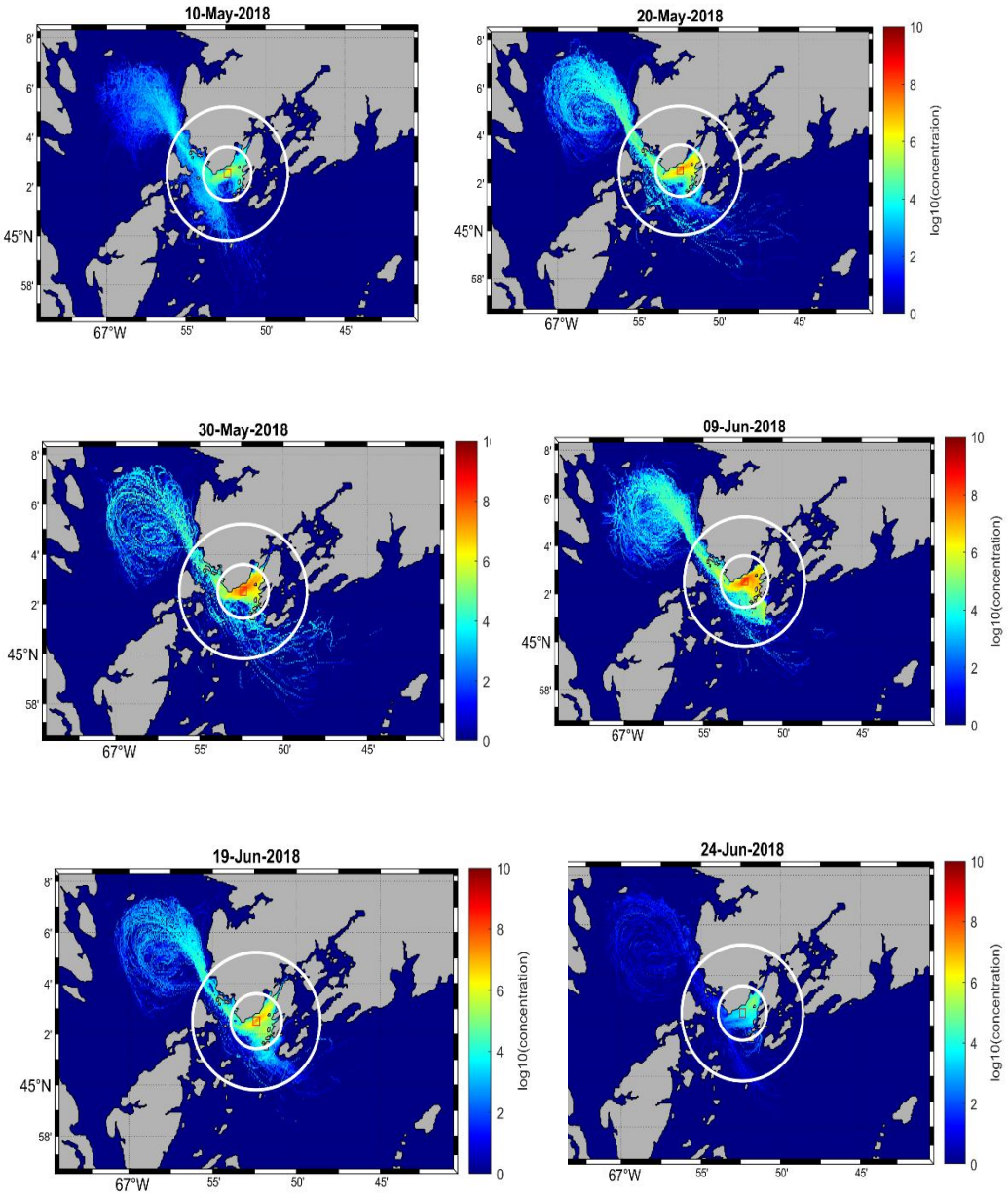
10-May-2018
20-May-2018
30-May-2018
09-Jun-2018
19-Jun-2018
24-Jun-2018
log10(concentration)
67°W
45°N

Fig. S7.1 ISAV concentration ($\log_{10}(TCID_{50}\ m^{-3})$) in the top 15 m of the water column and summed over a 24-h period on (10, 20, 30, 40, 50, and 55 days) post-outbreak, released from Farms 1 and 3-13. For each the red square represents the Farm's location. The radii of the two white circles centered at the Farms are 2 km and 5 km, respectively.

Supplementary Information 8. Tidal elevation in Passamaquoddy Bay and UV radiation.

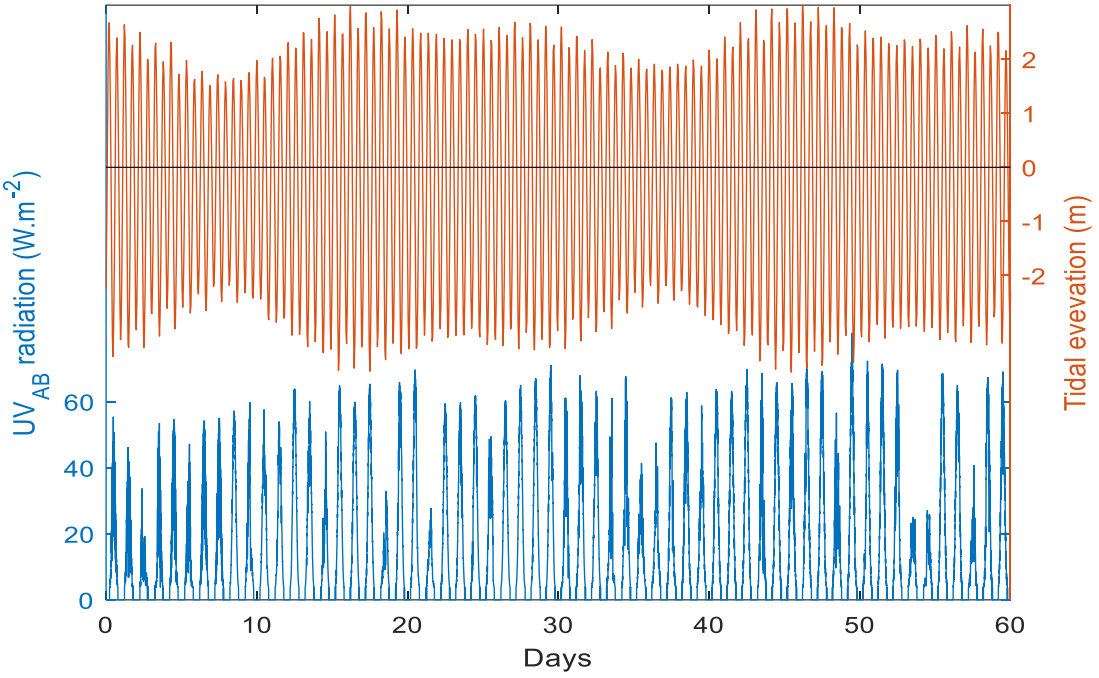

Fig. S8.1 Tidal elevation in Farm 2 from the ocean circulation module (red line) and UV_{AB} radiation (blue line) during May 1 to Jun 30, 2018.

Note: Ultraviolet (UV) index raw data is from the closest available UV monitoring station in Toronto, ON (Canada). Data available at: https://exp-studies.tor.ec.gc.ca/. The conversion method from UV index to UV_{AB} radiation is detailed in Supplementary Material.